Received: 8 November 2022 | Revised: 19 October 2023 | Accepted: 19 December 2023

DOI: 10.1002/we.2893

RESEARCH ARTICLE

WILEY

IPC-based robust disturbance accommodating control for load mitigation and speed regulation of wind turbines

Edwin Kipchirchir | **Dirk Söffker**

Dynamics and Control, University of Duisburg-Essen, Duisburg, Germany

Correspondence
Edwin Kipchirchir, Dynamics and Control, University of Duisburg-Essen, Duisburg, Germany.
Email: edwin.kipchirchir@uni-due.de

Present address
Edwin Kipchirchir, Duisburg, Lotharstr, 1,47057, Germany.

Funding information
German Academic Exchange Service (DAAD) scholarship

Summary

Over the past few decades, global demand for renewable energy has been rising steadily. To meet this demand, there has been an exponential growth in size of wind turbines (WTs) to capture more energy from wind. Consequent increase in weight and flexibility of WT components has led to increased structural loading, affecting reliability of these wind energy conversion systems. Spatio-temporal variation of rotor effective wind field acts as a disturbance to a WT system, hence, necessitating controllers that can cancel this disturbance. Additionally, assumptions made in extracting linear models for controller design lead to modeling errors resulting from changing operating conditions. Previous attempts have proposed robust controllers incorporating wind disturbance models. However, these controllers have been evaluated on smaller WTs, which experience lower structural loading than larger ones. Additionally, a majority these controllers are based on collective pitch control (CPC), hence do not address loading in the blades. To address these challenges, this contribution proposes an independent pitch-based robust disturbance accommodating controller (IPC-RDAC) for reducing structural loads and regulating generator speed in utility-scale WTs. The proposed controller is designed using μ-synthesis approach and is evaluated on the 5 MW National Renewable Energy Laboratory (NREL) reference WT. Its performance is evaluated against a gain-scheduled proportional integral (GSPI)-based reference open-source controller (ROSCO) and a CPC-based RDAC (CPC-RDAC) controller, developed previously by the authors. Simulation results for various wind conditions show that the proposed controller offers improved performance in blade and tower load mitigation, as well a generator speed regulation.

KEYWORDS
disturbance accommodating control, independent pitch control, load mitigation, robust control, wind turbine

1 | INTRODUCTION

Wind energy has been identified to play a key role in the energy transition to net-zero climate targets,[1] which is due to its higher capacity factor compared to other renewable sources.[2] The need to capture more energy from wind has led to a progressive increase in the size of wind turbines

(WTs) over the past few decades.[3] This has resulted in larger, heavier, and highly flexible rotors and towers. Coupled with stochastic wind inflow conditions, this has exacerbated fatigue loading of these structural components, consequently impacting reliability and increasing operation and maintenance (O&M) costs of WTs.

Several advanced control strategies have been proposed in recent years to reduce structural loads and optimize power production in WTs. However, due to hardware limitations, most industry controllers still rely on classical approaches such as proportional integral (PI) control.[4] In above-rated wind speed operation, collective pitch control (CPC), in which blades are pitched collectively, is used to regulate speed/power and reduce symmetrical loads in the tower and platform pitch motion in floating offshore WTs (FOWTs). For load reduction, individual control loops have been added to the classical CPC generator speed controller. However, coupling between different WT dynamics such as blade flap-wise (F-W)and tower fore-aft (F-A) modes with the drive-train can result in performance deterioration.[5] To damp periodic loads in rotor blades caused by unsymmetrical wind fields and gravitational force, independent pitch control (IPC) is required.[6]

Stochastic nature of wind is considered as a disturbance to a WT system. Consequently, there is need to reduce its effect on the performance of the turbine. Disturbance accommodating control (DAC) based on IPC has been proposed in earlier studies[7,8] for regulating rotor speed and reducing 1P asymmetrical blade F-W load in above-rated operation. In Menezes et al,[9] a CPC-based DAC controller is employed to actively damp tower F-A vibrations and regulate rotor speed in the 5 MW National Renewable Energy Laboratory (NREL) reference turbine. Unlike conventional DAC which relies on assumed waveform structured disturbances, a DAC controller is designed in Cheon et al[10] considering random process theories simulating stochastic wind conditions, for regulating rotor speed and alleviating fatigue load in above-rated operation. The proposed controller shows improved performance compared with CPC and IPC controllers. Although DAC controllers have been shown to improve performance in wind energy conversion systems by rejecting wind disturbance effects, they are not robust to model uncertainties and nonlinearities. For this, robust control methods need to be employed.

In recent years, robust control methods have received increasing interest in WT applications due to their inherent robustness to model uncertainties and system nonlinearities. Independent controllers synthesized using H_∞ optimization are applied to realize multi-objective control problems in earlier studies.[5,11,12] In Geyler and Caselitz,[5] two H_∞ controllers are designed and applied to an analytical model of a WT in above-rated zone. One CPC-based controller regulates generator speed and utilizes tower F-A acceleration displacement measurement to reduces first axial tower bending moments, while the other IPC-based controller reduces 1P blade oscillations. In earlier studies,[11,12] a set of two H_∞ multi-input single-output (MISO) controllers are proposed for above-rated operation of a 5 MW WT. A H_∞ controller is designed for generator speed control and load reduction in the tower, while a H_∞ generator torque controller reduces drive-train torsional load. Notable improvements are realized when compared with a baseline PI controller having a tower F-A damper and drive-train torque damper. A two degree of freedom (DOF) H_∞ controller is proposed in Poureh and Nobakhti,[13] for drive-train torsional damping on a 2 MW WT in full load region operation. Considerable robust performance (RP) is achieved when compared with a gain-scheduled PI (GSPI) and DAC controllers. Nevertheless, H_∞ control synthesis procedure is conservative given that plant uncertainties are not modeled. To obtain a robust controller for a plant having parametric and/or dynamic uncertainties, μ-synthesis approach which extends H_∞ optimization can be employed.[14] Robust controllers based on μ-synthesis using *DK*-iteration procedure have been proposed in previous studies.[6,15–17] In Mirzaei et al,[15] parametric uncertainties in the drive-train are considered in designing a robust controller for better regulation of generated power and rotor speed. However, its impact on the turbine's component loads is not studied. A robust μ-synthesis approach based on IPC is proposed in earlier research,[6,16] for reducing periodic blade F-W loads. In both cases, a CPC controller is designed as a separate loop for generator speed regulation. However, overall closed-loop optimality and stability are not investigated. Additionally, while this approach is promising, the effect of wind disturbances is not considered, and its impact on load channels which are highly coupled to the blades, like the tower F-A, is not investigated.

Nonlinear robust control methods such as sliding mode control (SMC) applied to WTs have been studied in earlier studies.[18–20] Given that SMC controllers suffer from chattering effect in the control input due to high-frequency switching, adaptive methods have been used to mitigate this phenomena. In Zhang et al,[18] a CPC-based adaptive robust controller based on high-order sliding mode (HOSM) is proposed for regulating rotor speed and reducing platform pitch motion of FOWTs. Although chattering effects are reduced, its effectiveness in structural load mitigation is not investigated. In Azizi et al,[19] adaptive output feedback SMC is employed with satisfactory results, to regulate the rotor speed and power on a 5 MW reference WT in the presence of uncertainties and actuator faults. A comparative study in Nayeh et al[20] focusing on SMC and H_∞ control designed via μ-synthesis concludes that SMC approach shows better tracking and transient performance albeit with slight chattering effect. In general, SMC has being employed in WTs mostly for regulation and tracking problems. However, its effectiveness in handling multi-objective control problems involving load mitigation has not been extensively studied.

In previous research,[21–23] a CPC-based robust DAC (RDAC) controller is implemented for generator speed regulation and tower load mitigation. Contrary to the DAC controllers proposed in earlier studies,[7–9] the disturbance observer, state feedback, and disturbance rejection gain matrices are synthesized simultaneously, hence ensuring overall system optimality and robustness. Additionally, compared with the aforementioned robust controllers, integration of a step disturbance model in control synthesis improves the rejection of persistent wind disturbance effects on the controlled outputs. The CPC-RDAC controller is designed using nonsmooth H_∞ synthesis approach. In Kipchirchir et al,[23] the developed mixed-sensitivity controller showed improved performance compared with the state-of-art reference open-source controller (ROSCO).[4] However, because CPC control is implemented, mitigation of periodic blade loads is not considered. Although simulation results show improved

disturbance rejection, uncertainties are assumed and not approximated; hence, the resulting controller might not be adequately robust. Therefore, there is need for an IPC-based robust controller that can reject wind disturbances with improved robustness to model uncertainties having an approximate description, to solve the multi-objective problem of speed regulation and load mitigation in commercial WTs. CPC can only reduce structural loading of components in the fixed reference frame, like the tower and drive-train. However, IPC control relies on multiblade coordinate (MBC) transformation[24] to transform blade dynamics in the rotating frame to the fixed frame; hence, both symmetric and asymmetric blade loads can be reduced.

This contribution proposes a novel IPC-based RDAC (IPC-RDAC) control scheme for structural load mitigation and generator speed regulation of commercial WTs in above-rated operation. It takes advantage of IPC to actively damp fatigue loading in both rotor blades and tower by compensating for asymmetrical wind inflow conditions. Unlike previous robust control attempts applied for mitigation of loads in WT rotor blades or towers, the proposed IPC approach alleviates fatigue loading in both the tower and blade structures. For controller design, the WT dynamics are modeled in OpenFAST using the 5 MW NREL reference WT.[25] The description of model uncertainties is derived from a family of plants, and μ-synthesis approach is used to design the proposed controller to be robust to these uncertainties and nonlinearities resulting from wind disturbances. Evaluation of simulation results for a variety of wind fields shows that the proposed controller exhibits better performance in structural load mitigation without trading off generator speed regulation compared with the baseline ROSCO controller[4] and the CPC-based RDAC (CPC-RDAC) controller.[23] The average blade F-W moments are reduced by 18.3 % and 23 % compared with ROSCO and CPC-RDAC controllers, respectively. The tower F-A moment is reduced by 9.8 % compared with ROSCO. The mean square error (MSE) in generator speed regulation is reduced by 51.5 % compared with ROSCO. In the worst-case scenario with the WT operating in wind conditions outside the control design working point, the proposed approach exhibits robustness in structural load reduction for all load channels while maintaining optimal generator speed regulation.

This contribution is organized as follows. In Section 2, the 5 MW NREL WT model and the baseline ROSCO and CPC-RDAC controllers, used to evaluate the performance of the proposed control strategy, are described. In Section 3, the IPC-RDAC controller design and implementation are outlined. In Section 4, results obtained from closed-loop dynamic simulation of the NREL 5 MW reference WT using various wind profiles are discussed. Finally, conclusions are drawn in Section 5.

2 | WT MODEL AND BASELINE CONTROLLER DESCRIPTION

2.1 | WT model

In the recent past, reference wind turbines (RWTs) have been used as a test-bed to study newly developed control technologies for improving performance of WTs.[26] In this contribution, the land-based 5 MW NREL RWT,[25] which is domicile in the high fidelity open-source fatigue, aerodynamics, structures, and turbulence (OpenFAST) software,[27] is chosen for designing and evaluating the closed-loop coupled dynamic response of the proposed control scheme. In Table 1, a summary of the three-bladed, upwind RWT is given. The 5 MW RWT model has 16 degrees of freedom (DoFs) describing the blades, tower, drive-train, generator, and nacelle motions. However, only six DoFs are enabled to capture the most important dynamics, corresponding to the desired closed-loop performance with respect to structural load mitigation and generator speed

TABLE 1 The 5 MW NREL reference wind turbine specifications.

Parameter	Value	Unit
Rated power	5	MW
Hub height	90	m
Cut-in, rated, cut-out wind speed	3, 11.4, 25	$m\,s^{-1}$
Cut-in, rated rotor speed	6.9, 12.1	rpm
Gearbox ratio	90	-
Rotor, hub radius	63,1.5	m
Blade pitch range	0-90	$^\circ$
Pitch rate	8	$^\circ\,s^{-1}$
Optimum pitch angle (β_{opt})	0	$^\circ$
Optimal tip-speed-ratio (λ_{opt})	7.55	-
Maximum power coefficient ($C_{p_{max}}$)	0.482	-

Abbreviation: NREL, National Renewable Energy Laboratory.

regulation. The enabled DoFs include first tower F-A bending mode, first blade F-W bending modes, drive-train rotational flexibility, and generator motion.

The nonlinear WT dynamics modeled in OpenFAST can be described using the generalized equation of motion expressed as

$$M(q,u,t)\ddot{q}+f(q,\dot{q},u,u_d,t)=0, \tag{1}$$

where M denotes the mass matrix, f a nonlinear forcing function of the enabled DoFs q and their first derivatives $\dot{q}$, as well as the control input u, wind disturbance input u_d, and time t.

The nonlinear model 1 is linearized in OpenFAST about a steady-state operating point in the above-rated wind speed region defined by a 18 m/s steady wind speed, 12.1 rpm rated rotor speed, and associated blade pitch angle of 14.6°. For the purpose of designing an independent pitch controller to mitigate periodic aerodynamic loading due to vertical wind shear, 36 equispaced azimuth positions are selected in the linearization process. The obtained 36 linear models, which capture this periodicity, are expressed in state-space form as

$$\begin{aligned}\dot{x}_m &= A_m(\psi)x_m + B_m(\psi)u_m + B_{d_m}(\psi)d\\ y_m &= C_m(\psi)x_m,\end{aligned} \tag{2}$$

where $A_m \in \mathbb{R}^{11x11}, B_m \in \mathbb{R}^{11x3}, B_{d_m} \in \mathbb{R}^{11x1}$, and $C_m \in \mathbb{R}^{4x11}$ denote the azimuth (ψ) -dependent system control input, disturbance, and output matrices, respectively, all of which are in the mixed coordinate frame. The perturbed independent pitch angles $[\Delta\beta_1\,\Delta\beta_2\,\Delta\beta_3]^T$ are denoted by $u_m \in \mathbb{R}^{3x1}$, and $d \in \mathbb{R}^{1x1}$ denotes the perturbed hub-height wind speed Δv. The measurements $y_m \in \mathbb{R}^{4x1}$ include generator speed ω_g and blade-root F-W bending moments ζ_1, ζ_2, and ζ_3. The dynamic states x_m include the enabled DoF displacements (besides generator displacement) and their respective velocities.

In OpenFAST, the dynamics of the rotor blades are expressed in the rotating coordinate frame. To model the coupled dynamics of the tower-nacelle sub-system expressed in the fixed frame and the spinning rotor, MBC transformation[24] is used to transform individual blade dynamics to the non-rotating frame. This transformation yields a model describing WT coupled dynamics in the fixed frame, effectively facilitating IPC controller design. After performing MBC transformation, the obtained azimuth-dependent reduced order models are averaged to obtain a weakly periodic linear model expressed as

$$\begin{aligned}\dot{x} &= Ax + Bu + B_d d\\ y &= Cx,\end{aligned} \tag{3}$$

where A, B, B_d, and C denote the system, input, disturbance, and output matrices, respectively. The measurements y include generator speed ω_g and the MBC transformed average, tilt, and, yaw blade-root F-W bending moments $\zeta_{avg}, \zeta_{tilt}$, and ζ_{yaw}, respectively. The linear time invariant model 3 is used to design the proposed IPC-RDAC controller.

The MBC transformation of the blade F-W moments from the rotating to the fixed frame is expressed as

$$\begin{bmatrix}\zeta_{avg}\\ \zeta_{tilt}\\ \zeta_{yaw}\end{bmatrix} = T(\psi)\begin{bmatrix}\zeta_1\\ \zeta_2\\ \zeta_3\end{bmatrix}, \tag{4}$$

with

$$T(\psi)=\frac{2}{3}\begin{bmatrix}\frac{1}{2} & \frac{1}{2} & \frac{1}{2}\\ \cos(\psi) & \cos\left(\psi+\frac{2}{3}\pi\right) & \cos\left(\psi+\frac{4}{3}\pi\right)\\ \sin(\psi) & \sin\left(\psi+\frac{2}{3}\pi\right) & \sin\left(\psi+\frac{4}{3}\pi\right)\end{bmatrix} \tag{5}$$

is the transformation matrix. Here, ζ_{avg} is the symmetric moment which is the average bending moments at the blade-roots caused by the out-of rotor plane flapping of the rotor blades in unison, while ζ_{tilt} and ζ_{yaw} are asymmetric moments induced by tilt and yaw motions, respectively.

2.2 | Baseline controllers

To evaluate the performance enhancement of the proposed control strategy, two CPC-based baseline controllers are used. The first is a recently developed modularized ROSCO controller[4] designed as a GSPI controller. The second one is a CPC-RDAC controller developed for the 5 MW NREL RWT.[23]

2.2.1 | Reference open-source controller

To keep up with the evolution of RWTs, over the past few decades the wind industry has experienced a growing need for baseline reference controllers. The ROSCO controller[4] was developed by NREL to be adaptable across different platforms of RWTs including the 5 MW NREL RWT. Only relevant control features are described for brevity. More details can be found in Abbas et al.[4] In Figure 1, a block diagram implementation of ROSCO controller logic is shown. A tip speed ratio (TSR) tracking generator torque control τ_g, which is suited to modern highly flexible rotors, is implemented in below-rated WT operation for maximum power extraction. On the other hand, to improve speed regulation performance, a GSPI collective blade pitch β controller is implemented in above-rated operation with the assumption of constant τ_g. Therefore, in steady-state operation, TSR is only a function of v; hence, an optimal pitch angle $\beta_{opt}(v)$ dependent on prevailing wind speed can be defined. Gain-scheduling is then realized using values of $\beta_{opt}(v)$ obtained from a power coefficient C_p curve of the 5 MW NREL RWT. The ROSCO controller has additional control features which reflect current trends in industry controller design. These include a pitch saturation, wind speed estimator, setpoint smoother, and floating feedback. Using a minimum blade pitch angle β_{min}, the pitch saturation module limits rotor thrusts near rated wind speed and maximizes power in the presence of rotor constraints in low wind speeds. A setpoint smoother avoids unwanted pitch and generator torque interactions near-rated operation using a shifting term $\Delta\omega$. A wind speed estimator is used for realizing TSR-tracking generator torque control and pitch saturation using a wind speed v. Tower-top pitch angle measurement ϕ is fed to the floating feedback module for platform stabilization in FOWTs using an additional pitch angle β_{float}. Although gain-scheduling greatly improves speed regulation performance in ROSCO, the controller does not account for modeling errors and system nonlinearities related to wind disturbance; hence, its performance is expected to deteriorate in case of changing operating conditions. Additionally, load mitigation is not implemented.

2.2.2 | CPC-based robust distance accommodating controller

A robust CPC controller is designed in Kipchirchir et al[23] for speed regulation and tower load mitigation of the 5 MW NREL WT in above-rated operation. The CPC-RDAC controller is robust against wind disturbance effects on the first tower F-A vibration mode.

The control system is formulated as a mixed-sensitivity H_∞ problem, which is then solved using non-smooth H_∞ synthesis.[28,29] In Figure 2, the CPC-RDAC controller applied to the 5 MW NREL RWT is shown. The incoming wind field d, which acts as a disturbance, excites the dynamics of the WT in above-rated operation. The generator speed ω_g and tower F-A bending moment ζ are the measured outputs fed to the observer-based control system RDAC, whose output is the CPC angle u used to regulate the WT's generator speed to its rated value $\omega_{g,rated}$ and reducing tower F-A vibration.

The weighting functions W_{11}, W_{12}, and W_2 are designed to achieve the requisite RP. To effect the required closed-loop generator speed response and improve robustness against wind disturbance, W_{11} is designed as an inverted high-pass filter. To reduce first mode tower F-A oscillation, W_{12} is designed as an inverted-notch filter centered at the vibration frequency. To specify desired control bandwidth and improve robustness, W_2 is designed as an inverted low-pass filter. A pitch actuator denoted as PA is modeled as a second-order low-pass filter to account for slow dynamics of the pitch actuator relative to other turbine dynamics.

The generalized plant P, containing the fixed elements of the control architecture is interconnected using lower linear fractional transformation (LFT) with the observer-based system RDAC, which contains the tunable controller gain matrices. Through nonsmooth H_∞ synthesis, a CPC-RDAC controller that minimizes the maximum singular value of the closed-loop system from the disturbance d to the controlled outputs $[z_1 z_2 z_2]^T$

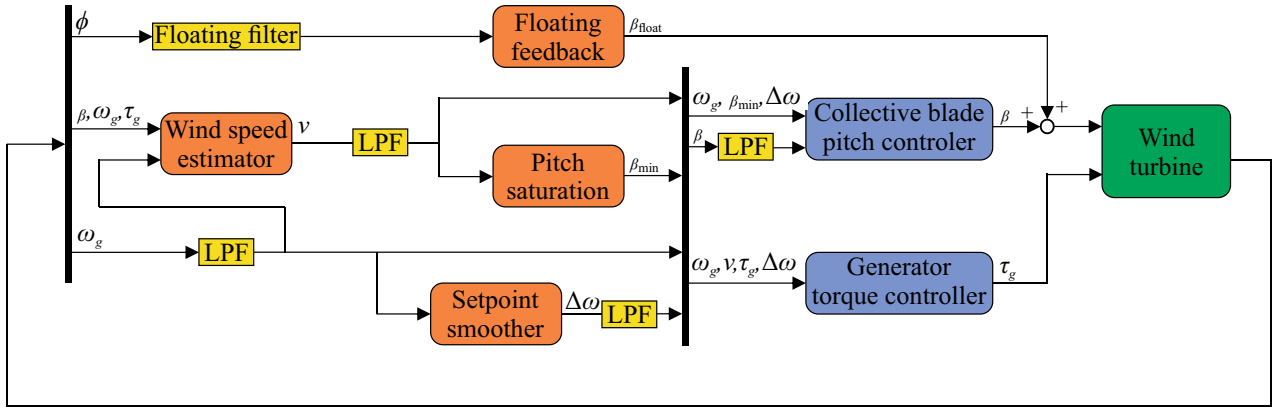

FIGURE 1 Block diagram of the general controller logic in reference open-source controller (ROSCO) (modified from Abbas et al.[4]).

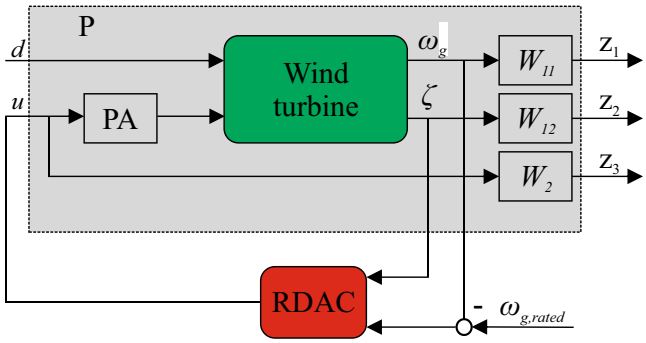

FIGURE 2 Robust disturbance accommodating controller (RDAC) applied to the 5 MW NREL reference wind turbine.

is obtained. It is shown through closed-loop dynamic simulations that the obtained CPC-RDAC controller improves generator speed regulation while reducing tower F-A vibration compared with ROSCO controller. However, in stochastic wind conditions, increased pitching activity leads to steady-state generator speed variations. Implementation of CPC control also means that load mitigation is only realized in the tower. Additionally, given that uncertainties are assumed and not modeled, the approach yields a controller with conservative robustness. Therefore, in this contribution, an IPC-RDAC controller is proposed. It incorporates uncertainty modeling using a family of linear models. In addition to the DAC control approach implemented in CPC-RDAC, regulating the generator speed and reducing persistent wind disturbances on the tower, the proposed controller uses blade load measurements in combination with MBC transformation to reduce periodic blade loads caused by vertical wind shear and gravitational loads. The blade dynamics are transformed from the rotating to the fixed frame. Using weighting functions, closed-loop frequency response of the symmetric and asymmetric blade F-W moments in the fixed frame is shaped at 3P frequency, hence reducing 2P, 3P, and 4P frequencies. The first tower F-A vibration mode is additionally reduced by designing notches at this frequency reflected on the assymetric blade moments.

3 | IPC-BASED ROBUST DAC

3.1 | DAC

Power quality and structural loading of WT components are strongly influenced by the turbulent conditions of the rotor effective wind speed variations. Therefore, there is a need to cancel or in the minimum reduce these wind disturbances without affected observability and full-state feedback. Assuming that the disturbance structure is known, model 2 can be augmented with an step wind disturbance model,[30] to design a DAC controller. Uniform variation in rotor effective wind speed is considered as an additive disturbance whose model is expressed as

$$\begin{aligned} d &= \theta x_d \\ \dot{x}_d &= F x_d, \end{aligned} \tag{6}$$

where x_d denotes the wind disturbance state and the disturbance state-space model is θ and F. A step disturbance with $\theta = 1$ and $F = 0$, closely approximates sudden uniform fluctuations in rotor effective wind speed,[31,32] and from a principal point of view appears in combination with high gains as a suitable practical solution,[33] for accommodating persistent wind disturbances.

Model 2 is augmented with the wind disturbance model 6 to obtain an extended linear model expressed as

$$\begin{aligned} \underbrace{\begin{bmatrix} \dot{x} \\ \dot{x}_d \end{bmatrix}}_{\dot{x}_a} &= \underbrace{\begin{bmatrix} A & B_d\theta \\ 0 & F \end{bmatrix}}_{A_a} \underbrace{\begin{bmatrix} x \\ x_d \end{bmatrix}}_{x_a} + \underbrace{\begin{bmatrix} B \\ 0 \end{bmatrix}}_{B_a} u \\ y &= \underbrace{\begin{bmatrix} C & 0 \end{bmatrix}}_{C_a} \begin{bmatrix} x \\ x_d \end{bmatrix}. \end{aligned} \tag{7}$$

To implement full-state feedback control, an extended observer used for estimating system and disturbance states is designed based on full observability of model 7. The observer is expressed as

$$\begin{aligned}\dot{\hat{x}}_a &= (A_a + B_a u - LC_a)\hat{x}_a + Ly \\ \hat{y} &= C_a \hat{x}_a,\end{aligned} \tag{8}$$

where $\hat{x}_a$ and $\hat{y}$ are the estimated states and measurements, respectively. Assuming (A_a, C_a) as observable, the observer gain matrix L can be designed using linear quadratic regulator (LQR) or pole placement methods. Appropriate design of L reduces estimation error $e = x_a - \hat{x}_a$ to zero. The estimated states $\hat{x}$ and $\hat{x}_d$ are used to implement full-state feedback control as

$$u = u_x + u_d = -(K_x \hat{x} + K_d \hat{x}_d), \tag{9}$$

where u_x realizes generator speed regulation and load mitigation objectives using the full-state feedback gain K_x, while u_d is used for disturbance rejection using the DAC gain K_d.

To regulate generator speed ω_g with no steady-state tracking error, the observer-based DAC model 8 is extended with an integral state $x_i = \int \omega_g dt$. This yields the partial integral action $\dot{x}_i = C_i y$, where C_i defines the location of generator speed in the output measurements. Although Kronecker product method can eliminate this tracking error, in this work, K_d is designed simultaneously together with the other gains in a single H_∞ optimization loop. Therefore, the extended observer-based DAC model becomes

$$\begin{aligned}\underbrace{\begin{bmatrix}\dot{\hat{x}}_a \\ \dot{x}_i\end{bmatrix}}_{\dot{x}_b} &= \underbrace{\begin{bmatrix}A_a - B_a K_a - LC_a & -B_a K_i \\ 0 & 0\end{bmatrix}}_{A_b} \underbrace{\begin{bmatrix}\hat{x}_a \\ x_i\end{bmatrix}}_{x_b} + \underbrace{\begin{bmatrix}L \\ C_i\end{bmatrix}}_{B_b} y, \\ u &= \underbrace{-\begin{bmatrix}K_x & K_d & K_i\end{bmatrix}}_{C_b} \begin{bmatrix}\hat{x} \\ \hat{x}_d \\ x_i\end{bmatrix},\end{aligned} \tag{10}$$

with K_i denoting the integral gain. Classical approaches including LQR and pole placement can be used for designing L, K_x, and K_i , while K_d can be designed separately using known methods such as Moore–Penrose pseudoinverse($\dagger$) and Kronecker product.[7,8,22] Separate design of the different gain matrices affects the state and disturbance estimation quality as full system optimality, and robustness is not considered or guaranteed. Additionally, model-system mismatch introduces uncertainties which affects closed-loop robustness. In this contribution, a robust H_∞ control method is used for designing these gains simultaneously, achieving the desired robustness and performance.

3.2 | Open-loop response of the WT model

The linear model 3 from MBC transformation is obtained from a specific operating point. However, it is expected that model uncertainties exist during operation due to variations in WT dynamics outside the design operating point of 18 m/s hub-height wind speed. Therefore, this uncertain behavior needs to modeled. This is illustrated in Figure 3 where the range of open-loop frequency response behavior is captured using a sample of linear models obtained from a selection of operating points defined by 14, 16, 20, and 22 m/s wind speeds. In this contribution, only these frequency-dependent unstructured uncertainties resulting from unmodeled dynamics related to changes in turbine operating points are considered. Parametric uncertainties, usually present at low frequencies because of plant perturbations,[5] are not considered.

The average (CPC) pitch command β_{avg} strongly influences generator speed ω_g and the average blade F-W moment ζ_{avg} as seen in larger magnitudes of the related frequencies. It also has a strong influence on the first tower F-A frequency as reflected by the response peaks of ζ_{tilt} and ζ_{yaw} blade moments at 2.07 rad/s. The β_{tilt} and β_{yaw} pitch commands, which are responsible for mitigating asymmetrical loading of blades, have a larger influence on ζ_{tilt} and ζ_{yaw} moments, respectively. Given the differences between the frequency responses of the nominal model and the uncertain models especially in high frequencies above the rated rotor speed $\omega_r = 1.267$ rad/s, relying only on the nominal model obtained at 18 m/s would lead to high model-system mismatch. In this contribution, wind disturbances are assumed to generate additive uncertainty because the frequency responses of the family of uncertain plants produce modest variability as compared with the nominal model. Therefore, these frequency responses are modeled using unstructured additive uncertainty and combined with the nominal WT plant G (3), hence obtaining an uncertain plant $\tilde{G}$ of the form

$$\tilde{G} = G + W\Delta_a, \tag{11}$$

where Δ_a denotes the uncertain dynamics with unit peak gain and W denotes a 4×4 diagonal shaping filter. The orders of each of the diagonal elements are designed to adjust the amount of uncertainty at each frequency. This ensures that the gaps between the nominal and uncertain models are closely tracked, hence improving uncertainty estimation. In this work, the orders of each diagonal entry of W are designed to shape

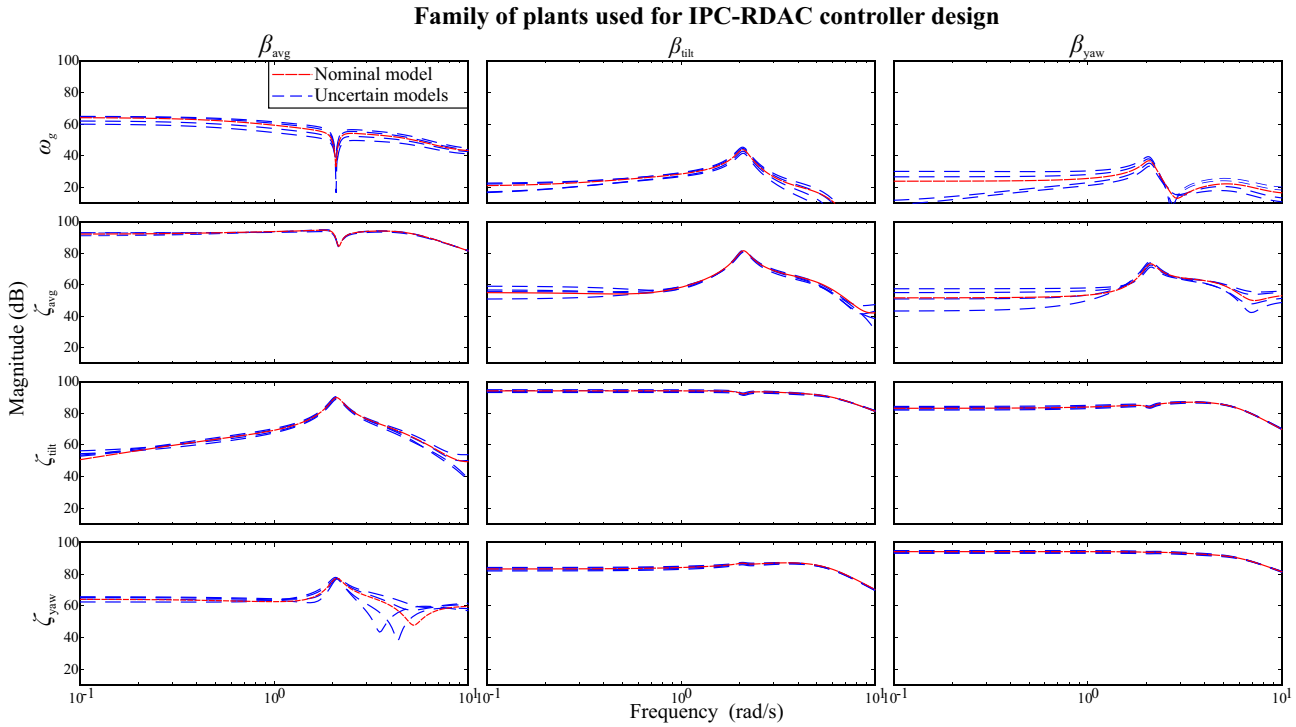

FIGURE 3 Comparison of open-loop frequency responses from pitch commands to measured outputs between nominal model and uncertain models.

the uncertainty in the respective outputs y of the family of uncertain plants. The obtained uncertainty $\Delta = W\Delta_a$, which has a 4×4 block diagonal structure, is used for designing the proposed IPC-RDAC controller.

In this contribution the robust H_∞ control approach based on μ-synthesis is used to design the IPC-RDAC controller for load mitigation and speed regulation in the 5 MW NREL RWT.

3.3 | Mixed sensitivity H_∞ control background

The standard H_∞ controller is used to design an optimized controller R^* that minimizes the maximum singular value, that is, the H_∞ norm $\|.\|_\infty$ of a transfer function G_{zd} from exogenous disturbance d to controlled outputs z. It is expressed as

$$R^* = \underset{R \in \mathcal{R}}{argmin} \|G_{zd}(P,R)\|_\infty, \tag{12}$$

where $\mathcal{R}$ denotes a set of all controllers R that stabilize the nominal plant P. The standard robust controller can be solved using algebraic Riccati equations (AREs) or linear matrix inequalities (LMIs).

The standard H_∞ control approach cannot be applied for the design of the observer-based DAC control system 10 given that it has structural constraints related to its control gains L, K_a, and K_i. To achieve the required trade-off between control effort and performance, weighting functions are usually introduced to the nominal plant P, leading to a mixed-sensitivity H_∞ control problem expressed as

$$R^* = \underset{R \in \mathcal{R}}{argmin} \left\| \begin{matrix} W_1 S \\ W_2 RS \\ W_3 T \end{matrix} \right\|_\infty, \tag{13}$$

where S, RS, and T denote the sensitivity, control sensitivity, and complementary sensitivity functions, respectively. The weighting functions denoted by W_1, W_2, and W_3 specify the target closed-loop frequency responses of the respective sensitivity functions.

The mixed-sensitivity H_∞ control approach 13 serves as a cost function for optimizing parameters of the observer-based DAC controller 10. The problem to find an optimal RDAC controller $RDAC^*(L,K)$ defining the optimal gains $K=[K_x K_d K_i]$ and $L=[LC_i]^T$ is formulated as

$$RDAC^* = \underset{RDAC \in \mathcal{RDAC}}{argmin} \|G_{zd}(P,RDAC)\|_\infty, \tag{14}$$

where $\mathcal{RDAC}$ denotes a set of controllers *RDAC* that stabilize the generalized plant *P*.

To guarantee the asymptotic stability of the closed-loop system, the optimization problem 14 is subjected to Lyapunov stability constraint given as $\|C_b(sI-\mathcal{A}(RDAC))^{-1}B_b\|_\infty < +\infty$, where $\mathcal{A}(RDAC)$ denotes the closed-loop system matrix A_b. Therefore, the optimization problem becomes

$$\begin{aligned} RDAC^* &= \underset{RDAC \in \mathcal{RDAC}}{argmin} \|G_{zd}(P,RDAC)\|_\infty \\ s.t.\ &\|C_b(sI-\mathcal{A}(RDAC))^{-1}B_b\|_\infty < +\infty. \end{aligned} \tag{15}$$

In this contribution, nonsmooth μ-synthesis approach[34] is used for the design of an optimal IPC-RDAC controller.

3.4 | IPC-based robust DAC approach applied to the 5 MW NREL reference WT

3.4.1 | Proposed control structure

The proposed IPC-RDAC controller is applied and therefore used to control the 5 MW NREL RWT as shown in Figure 4. The model-system mismatch due to variations in operating point is modeled as unstructured additive uncertainty Δ. Wind disturbance *d* excites the WT dynamics in above-rated operation. The generalized plant P, which is made up of a combination of nominal WT plant, pitch actuator PA, and weighting functions W_{xy}, is interconnected with the observer-based IPC-RDAC system 15 using lower LFT, and Δ using upper LFT. The controlled outputs $z=[z1z2z3z4z5z6z7]^T$ consist of the weighted generator speed, average, tilt, and yaw blade F-W bending moments, and weighted control signals. The IPC-RDAC controller relies on the generator speed ω_g and the MBC transformed blade F-W bending moments $\zeta_{avg}, \zeta_{tilt}$, and ζ_{yaw} to generate independent pitch angles $[\beta_{avg}\beta_{tilt}\beta_{yaw}]^T$. Inverse MBC transformation matrix $T(\psi)^{-1}$ transforms these control signals back to the rotating coordinate system to obtain IPC signals *u*. The optimal H_∞ structured controller RDAC is designed using *DK*-iteration process based on μ-synthesis by minimizing the structured singular value (SSV) μ.

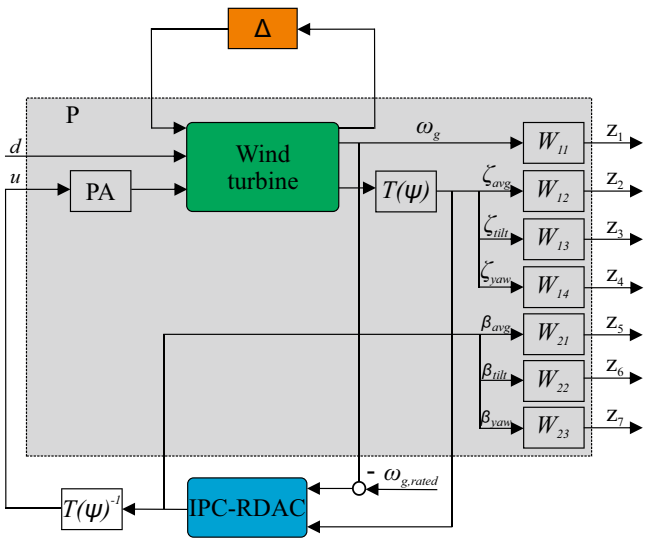

FIGURE 4 Block configuration of independent pitch-based robust disturbance accommodating controller (IPC-RDAC) controller applied to the 5 MW National Renewable Energy Laboratory (NREL) reference wind turbine.

To account for slow pitch actuator dynamics relative to other turbine dynamics, the WT model is supplemented with a pitch actuator for each blade, which is modeled as a second-order transfer function from the commanded individual pitch angle β_{com} to the actual pitch angle β. It is expressed as

$$\beta = \frac{\omega_{PA}^2}{s^2 + 2\zeta\omega_{PA}s + \omega_{PA}^2}\beta_{com}, \tag{16}$$

where ω_{PA} denotes the natural frequency taken to be four times the turbine's rated rotor speed $\omega_r = 1.267$ rad/s and ζ is the damping ratio which is 80% critical as recommended by NREL.[35] The individual pitch angles are used for regulating generator speed to its rated value $\omega_{g,rated}$ and for damping the first tower F-A vibration mode and assymetric blade F-W vibrations, which include tilt and yaw F-W motions. This reduces the tower F-A load and damps the asymmetrical blade F-W loading at 2P, 3P, and 4P frequencies. This is realized by designing suitable weighting functions.

3.4.2 | Weighting function selection

Periodic loading of WT structures is manifested as harmonics of the rotor frequency. The MBC transformation converts the 1P, 2P, 3P,... frequencies in the rotating frame to 0P, 3P, 6P,... frequencies in the fixed frame as shown in Table 2. In this contribution, 2P, 3P, and 4P frequencies in the rotating frame are counteracted by designing appropriate weighting functions for shaping the respective closed-loop transfer function from the wind disturbance d to blade F-W bending moments $\zeta_{avg}, \zeta_{tilt}$, and ζ_{yaw}. Reduction at the stated frequencies is considered as these are close to the natural frequencies of the blades and tower. Due to the blade pitch actuator bandwidth limitation, frequencies beyond 4P are usually not considered in turbine control design.

To design the weighting functions, knowledge of the natural frequencies of the blades and tower components at different modes of vibration is crucial. The natural frequencies of the 5 MW NREL RWT are given in Table 3. Given that RP heavily relies on the weighting function selection, the closed-loop characteristics are shaped using the desired weighting functions which are rational, stable, and minimum phase.[36] Therefore, the frequency-dependent weighting functions $W_{11}, W_{12}, W_{13}, W_{14}, W_{21}, W_{22}$, and W_{23} are designed and imposed on respective measurement signals or system inputs to achieve the desired closed-loop frequency response. To effect the generator speed response and to ensure robustness against wind disturbances, W_{11} is designed as an inverted low-pass filter with the frequency at which W_{11}^{-1} crosses the open-loop response being adjusted to 0.1396 rad/s, which corresponds to the turbine's maximum pitch rate (PR), hence avoids violation of the turbines PR constraint.[5] To reduce vibrations in the tower and rotor blades, W_{12}, W_{13}, and W_{14} are designed as inverted notch filters centered at the respective frequencies. To reduce vibration at 3P frequency (3.8 rad/s) in both the fixed and rotating frames, the notch in filter W_{12} is centered at the 3P frequency. Filters W_{13} and W_{14} have two notches centered at the first tower F-A frequency (2.07 rad/s) and at 3P frequency, which corresponds to the 2P, 3P, and 4P frequencies in the rotating frame. To reduce the controller activity in high frequencies thereby increasing robustness by limiting the control bandwidth, filters W_{21}, W_{22}, and W_{23} are designed as inverted low-pass filters.

The weighting functions are integrated to the linear WT model as illustrated in Figure 4. Finally, this results in the three control inputs $u = [\beta_{avg}\beta_{tilt}\beta_{yaw}]^T$ and the four performance outputs $\omega_g, \zeta_{avg}, \zeta_{tilt}$, and ζ_{yaw}. The weighting functions W_{12}, W_{13}, and W_{14} are chosen as

$$W_{11} = \frac{\frac{s}{M_s} + \omega_s}{s + \omega_s\epsilon_s}, W_{12} = \left(\frac{s^2 + 2\alpha_1\omega_{3P}s + \omega_{3P}^2}{s^2 + 2\beta_1\omega_{3P}s + \omega_{3P}^2}\right) \times \frac{1}{522.6}, \tag{17}$$

$$W_{13} = \left(\frac{s^2 + 2\alpha_{21}\omega_{3P}s + \omega_{3P}^2}{s^2 + 2\beta_{21}\omega_{3P}s + \omega_{3P}^2}\right) \times \left(\frac{s^2 + 2\alpha_{22}\omega_{tfa}s + \omega_{tfa}^2}{s^2 + 2\beta_{22}\omega_{tfa}s + \omega_{tfa}^2}\right) \times \frac{1}{115.8}, \tag{18}$$

TABLE 2 Correspondence of harmonics in rotating and fixed frames.

Rotating frame	Fixed frame
1P	0P @ ζ_{tilt} and ζ_{yaw}
2P	3P @ ζ_{tilt} and ζ_{yaw}
3P	3P @ ζ_{avg}
4P	3P @ ζ_{tilt} and ζ_{yaw}
5P	6P @ ζ_{tilt} and ζ_{yaw}
6P	6P @ ζ_{avg}
7P	6P @ ζ_{tilt} and ζ_{yaw}

TABLE 3 Natural frequencies for the 5 MW NREL RWT.[25]

Vibration mode	Frequency (rad/s)
First blade asymmetric flap-wise yaw	4.187
First blade asymmetric flap-wise tilt	4.194
First blade symmetric flap-wise average	4.394
First blade asymmetric edge-wise yaw	6.781
First blade asymmetric edge-wise tilt	6.847
First tower fore-aft	2.036
First tower side-side	1.960
First drive-train torsion	3.899

Abbreviations: NREL, National Renewable Energy Laboratory.

$$W_{14} = \left(\frac{s^2 + 2\alpha_{31}\omega_{3P}s + \omega_{3P}^2}{s^2 + 2\beta_{31}\omega_{3P}s + \omega_{3P}^2}\right) \times \left(\frac{s^2 + 2\alpha_{32}\omega_{tfa}s + \omega_{tfa}^2}{s^2 + 2\beta_{32}\omega_{tfa}s + \omega_{tfa}^2}\right) \times \frac{1}{31.6}, \tag{19}$$

and

$$W_{21} = W_{22} = W_{22} = \frac{s + \frac{\omega_u}{\epsilon_u}}{s + \frac{\omega_u}{M_u}}, \tag{20}$$

where $Ms, \omega_s, \epsilon_s, \alpha_1, \beta_1, \alpha_{21}, \beta_{21}, \alpha_{22}, \beta_{22}, \alpha_{31}, \beta_{31}, \alpha_{32}, \beta_{32}, M_u, \omega_u,$ and ϵ_u are tuning parameters of the respective inverted weighting filters and $0 < \beta < \alpha < 1$.

In Figure 5, a Bode diagram of the open-loop transfer functions from wind speed to respective outputs and the related inverse weighting functions is shown. As illustrated, $1/W_{11}, 1/W_{12}, 1/W_{13}$, and $1/W_{14}$ shape the respective open-loop responses to achieve the desired closed-loop frequency responses.

3.4.3 | IPC-RDAC control design based on μ-synthesis

The performance of the observer-based control system shown in Figure 5 is assessed using the H_∞ norms of the weighted closed-loop transfer function G_{zd} from the wind disturbance d to the controlled outputs z, which should satisfy the performance given as

$$\|G_{zd}\|_\infty = \max_{\omega \in R} \bar{\sigma}(G_{zd}(j\omega)) \leq 1, \tag{21}$$

where $\bar{\sigma}$ is the maximum singular value.

From Figure 4, the upper LFT $F_u(M, \Delta)$ is made up of the transfer function M from the output to the input of the perturbation Δ, both of which are stable. The lower LFT $N = F_l(P, IPC - RDAC)$ interconnects the generalized plant P with the controller $IPC - RDAC$. Robust stability (RS) implies that an IPC-RDAC controller obtainable if the system remains stable for all family of plants shown in Figure 2. RP is guaranteed if the performance objective can be achieved for all possible plants in the uncertainty set, including the worst-case plant, and additionally, the RS condition is satisfied. While the M-Δ structure is used to analyze RS of the uncertain system, the N-Δ structure is used for RP analysis. Robust stability and performance criteria are expressed as

$$RS \Leftrightarrow F_u(M, \Delta) \text{ is stable for } \forall \Delta, \|\Delta\|_\infty \leq 1; \text{and NS}, \tag{22}$$

$$RP \Leftrightarrow \|F_l(N, \Delta)\|_\infty < 1 \text{ for } \forall \Delta, \|\Delta\|_\infty \leq 1; \text{and NS}, \tag{23}$$

where NS denotes nominal stability.

From small gain theorem,

$$RS \Leftarrow \bar{\sigma}(M) < 1 \, \forall \omega, \tag{24}$$

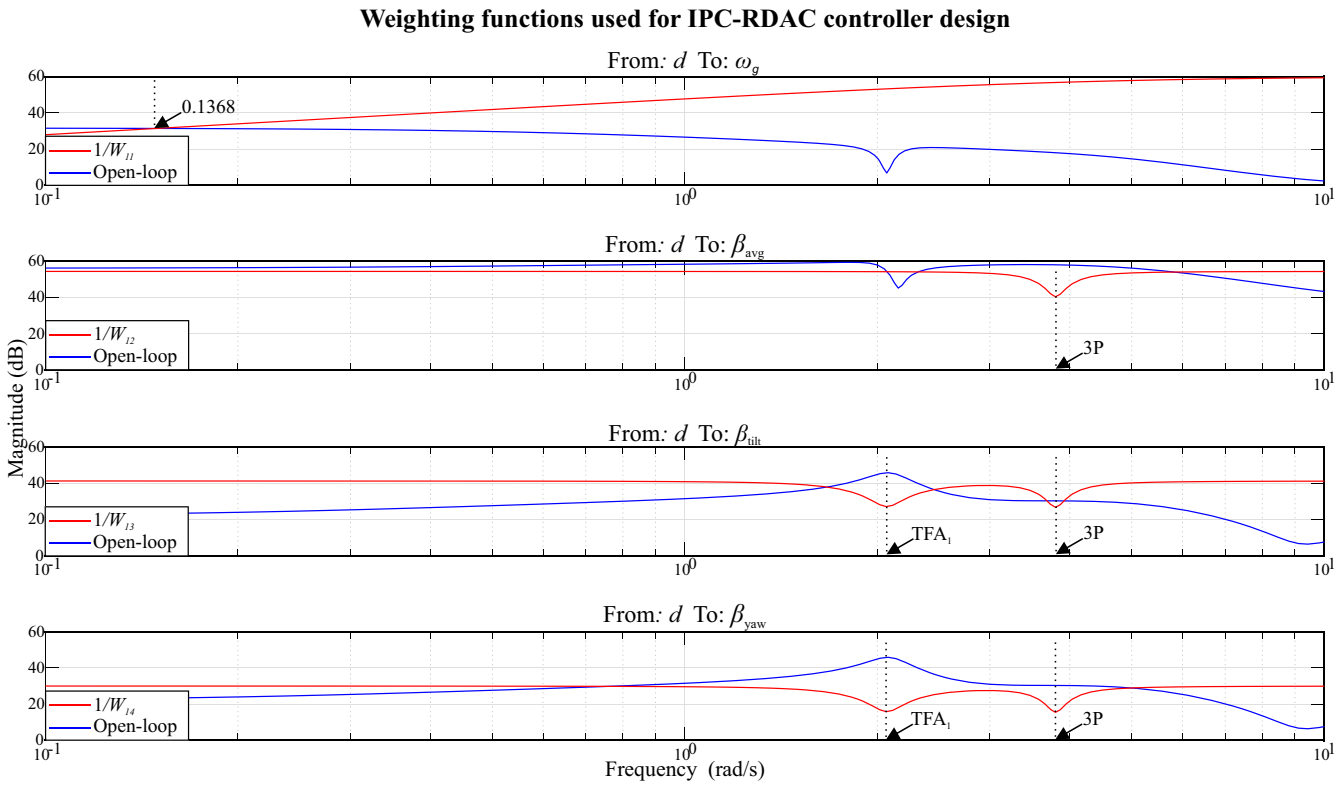

FIGURE 5 Comparison of open-loop frequency response and weighting functions used in independent pitch-based robust disturbance accommodating controller (IPC-RDAC) control design.

which is a tight condition for any case of complex Δ satisfying $\bar{\sigma} \le 1$. A more general tight condition is given as

$$RS \Leftrightarrow \mu(M) < 1 \forall \omega, \tag{25}$$

where the real nonnegative $\mu(M)$ is the SSV which is expressed as

$$\mu(M) = \frac{1}{\min\{k_m | \det(I - k_m M\Delta) = 0}, \tag{26}$$

for structured $\Delta, \bar{\sigma} \le 1$. If no structured uncertainty Δ exists, then $\mu(M) = 0$. The factor k_m is used to scale the uncertainty Δ to make the matrix $I - k_m M\Delta$ singular; hence, the SSV is expressed as $\mu(M) = 1/k_m$.[36]

In addition to the definition given in 23 which is given in terms of H_∞, RP can further be defined as a special case of RS given as

$$RP \Leftrightarrow \mu_{\hat{\Delta}}(N) < 1 \forall \omega, \hat{\Delta} = \begin{bmatrix} \Delta & 0 \\ 0 & \Delta_p \end{bmatrix}, \tag{27}$$

where Δ_p is a full complex perturbation representing the H_∞ performance bound across the disturbance/controlled outputs channel and has a block diagonal structure with dimension $n_d \times n_z$.

From the foregoing discussion, μ is a powerful RP analysis tool. However, for synthesizing a controller to minimize a certain μ condition, a scaled version of μ is needed.[15] The μ-synthesis based on *DK*-iteration process is used in this work to synthesize an optimal IPC-RDAC controller for the closed system, which minimizes the SSV μ while guaranteeing RP and RS. The process solves a sequence of scaled H_∞ problems by utilizing frequency-dependent scaling matrices, *D* and *G*, which take advantage of the uncertainty structure. First, nonsmooth H_∞ synthesis[29] finds an IPC-RDAC controller that minimizes the closed-loop gain of plant P. The process is summarized as

$$\min_{RDAC}\left(\min_{D\in\mathcal{D}}\|DN(IPC-RDAC)D^{-1}\|_{\infty}\right). \tag{28}$$

In the D-step, the robust H_∞ performance of the closed-loop system using the current IPC-RDAC controller is estimated. The upper bound $\overline{\mu}$ of the robust H_∞ performance of IPC-RDAC is then computed using suitable $D(j\omega)$ scaling which commutes with Δ. Rational functions $D(s)$ of a specified order are used to fit the $D(j\omega)$ scaling, yielding the scaled H_∞ norm μ_F. In the K step, a scaled controller $IPC-RDAC^*$ that minimizes μ_F to improve the RP obtained in the D-step is synthesized. The iterative process is repeated until no further improvement in μ is achievable by $IPC-RDAC^*$ within a specified tolerance. In this contribution, D scaling is used because the wind disturbance is assumed to produce complex additive uncertainty.

4 | RESULTS AND DISCUSSION

To validate the proposed control method, closed-loop dynamic simulations are performed in OpenFAST design code using the 5 MW NREL RWT. While the controller is designed using a reduced order (linearized) model of the WT, a nonlinear model is used in the simulations. This allows for the evaluation of control performance in the presence of modeling errors. The objectives of the proposed IPC-RDAC control scheme include regulation of generator speed to its rated value of 1173.7 rpm and reduction of structural loading in the blades (F-W mode) and the tower (F-A mode). To excite the dynamics of the WT in above-rated operation, stochastic wind fields are used. The performance of the proposed IPC-RDAC controller is evaluated against both the baseline ROSCO and CPC-RDAC controllers using closed-loop simulation results. The obtained results are analyzed and discussed using selected performance metrics.

4.1 | Structural load mitigation performance

A WT experiences spatio-temporal variations in the wind field acting on its rotor. To simulate the nonstationary wind conditions, stochastic wind profiles generated using TurbSim software[37] are used in closed-loop dynamic simulations. In Figure 6A, the full-field wind profiles generated using the international electro-technical commission (IEC) Kaimal spectral model are shown. Following the recommendation of the IEC 61400-1 standard for design load case (DLC) 1.2, which is related to fatigue load evaluation in WT structures, the 10 min long wind profiles are generated with different combinations of mean wind speeds, turbulence intensities (TIs), and random seeds. This covers most of the turbine's above-rated operation.

In Figure 6B, the closed-loop blade F-W load mitigation response of the WT is shown. As illustrated, the proposed IPC-RDAC controller shows improved performance in reducing the blade F-W bending moments in all wind field scenarios compared with the baseline ROSCO and CPC-RDAC controllers. This performance is attributed to reduction in 2P, 3P, and 4P blades loads using IPC control signals. In Table 4, load mitigation performance in the blade F-W and tower F-A load channels for all wind fields is given. The proposed IPC-RDAC controller reduces the average standard deviation δ in blade F-W bending moment by 9.8% compared with ROSCO. However, CPC-RDAC shows the worst performance with δ increasing by 6.1% compared with ROSCO. The performance in tower F-A load reduction is shown in Figure 6C. The proposed controller realizes improved tower F-A load mitigation performance compared with ROSCO as δ reduces by 9.8 % as shown in 4. The CPC-RDAC controller exhibits superior performance as δ reduces by 14.8 % compared with ROSCO. This is attributed to less control objectives compared with IPC-RDAC, as it only trades off tower F-A load mitigation and generator speed regulation. However, at lower mean wind speed of 14 m/s (treated as worst-case scenario), which is outside the 18 m/s control design working point and has a higher occurrence probability in real-world turbine operation, IPC-RDAC achieves the best performance in both load channels, hence proving its robustness to model uncertainties. Therefore, the proposed controller realizes optimal performance in mitigating both the blade F-W and tower F-A loads.

4.2 | Generator speed and power regulation performance

Given that the proposed controller is designed for structural load reduction and generator speed regulation, there is a need to ascertain that the foregoing improvement in load mitigation does not lead to deteriorated generator speed and power regulation performance. Therefore, the proposed IPC-RDAC controller is compared with the ROSCO and CPC-RDAC controllers as illustrated in Figure 7. Due to additional blade load mitigation control objective, the IPC-RDAC controller has slightly higher pitch usage as shown in Figure 7A. Compared with both ROSCO and CPC-RDAC, the proposed controller achieves improved generator speed regulation as illustrated in Figure 7B. In Table 5, the performance analysis

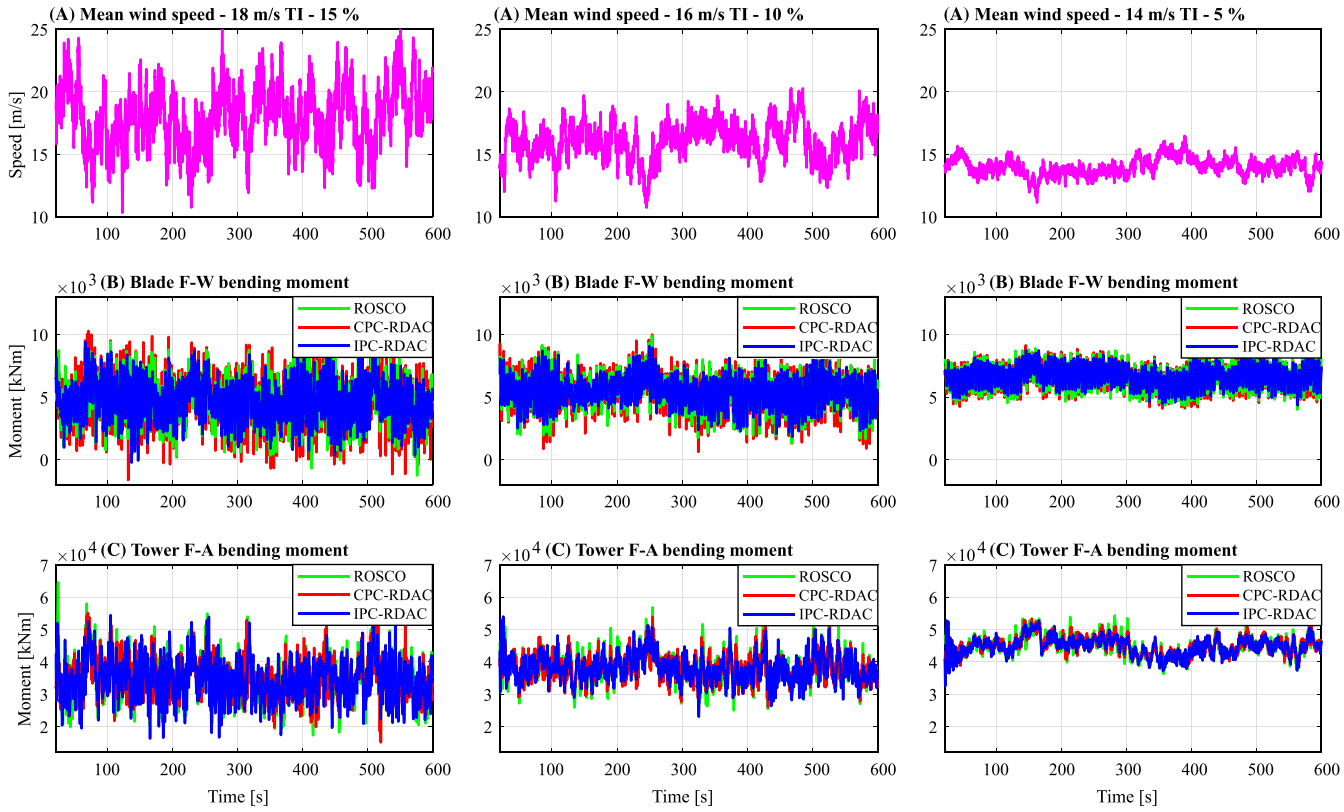

FIGURE 6 (A–C) Blade F-W and tower F-A load mitigation response.

TABLE 4 Blade F-W and tower F-A load mitigation performance analysis (Key: best, worst).

Load channel (kNm)	Controller	18 m/s	16 m/s	14 m/s	Avg.	%
Blade F-W (δ)	ROSCO	1805.8	1375.2	988.8	1389.9	-
	CPC-RDAC	1972.8	1450.7	998.8	1474.1	6.1
	IPC-RDAC	1494.3	1118.8	792.95	1135.35	−18.3
Tower F-A (δ)	ROSCO	6632.5	4758.7	3013	4801.4	-
	CPC-RDAC	5610.4	3948.9	2706.9	4088.7	−14.8
	IPC-RDAC	6277.9	4019.7	2697.7	4331.8	−9.8

Abbreviations: CPC-RDAC, CPC-based robust disturbance accommodating controller; IPC-RDAC, independent pitch-based robust disturbance accommodating controller.

in blade pitch usage and generator speed and power regulation for all wind fields is given. As shown, both CPC-RDAC and IPC-RDAC realize reduction in the average δ in generator speed by 34.9% and 26.6%, respectively, compared with ROSCO. This performance is also reflected in the MSE values. In comparison with ROSCO, the average generator speed MSE reduces by 62.5% and 51.5% for CPC-RDAC and proposed controllers, respectively. However, from Figure 7C, it is clear that ROSCO achieves superior power regulation performance, with the generator power δ increasing by 59% and 31.8% for CPC-RDAC and IPC-RDAC, respectively, compared with ROSCO as shown in Table 5. A similar performance is also reflected in generator power MSE. Therefore, although CPC-RDAC has superior speed regulation performance, this comes at a penalty as it achieves the worst power regulation. However, the proposed controller achieves an optimal compromise between generator speed and power regulation. The mean blade pitch travel is used to evaluate the controllers' blade pitch actuator usage for all wind fields as shown in Table 5. The proposed controller shows a marginal increase in pitch actuator usage compared with both ROSCO and CPC-RDAC.

In Figure 8, the average normalized values of blade PR RMS and generator speed and power regulation MSE obtained from simulation results for all wind fields are shown. To ascertain that blade pitch actuation does not violate the maximum PR of 8°/s for the 5 MW NREL RWT, the average PR root mean square (RMS) is evaluated and found to be 0.37°/s, 4.78°/s, and 7.78°/s for ROSCO, CPC-RDAC, and IPC-RDAC controllers, respectively. Due to additional control objective of blade and tower load mitigation, the proposed IPC-RDAC controller shows to significant pitch

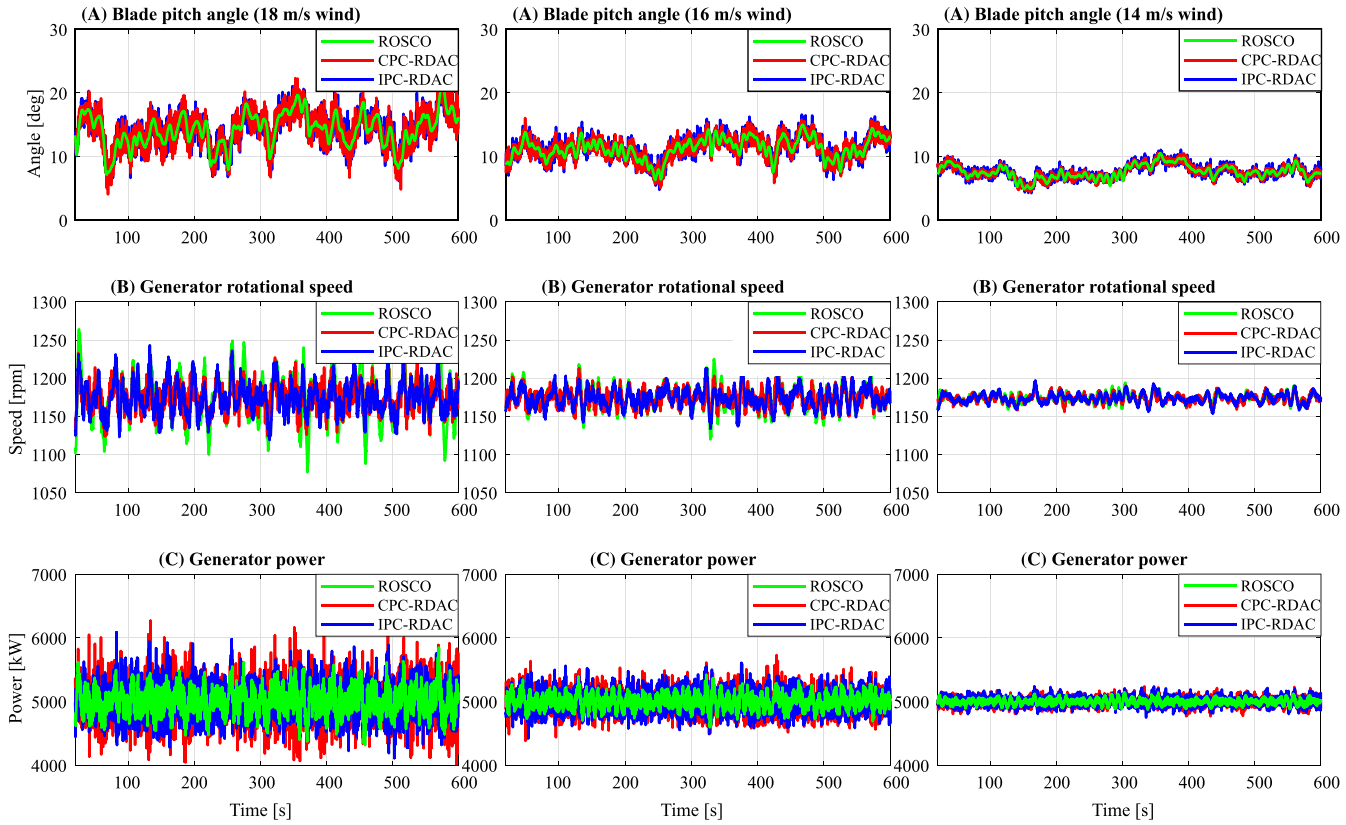

FIGURE 7 Generator speed and power regulation response.

TABLE 5 Blade pitch usage and generator speed and power regulation performance analysis (Key: best, worst).

Parameter	Units	Controller	18 m/s	16 m/s	14 m/s	Avg.	%
Generator speed (δ)	rpm	ROSCO	30.67	15.79	6.04	17.5	-
		CPC-RDAC	17.54	11.07	5.56	11.39	−34.9
		IPC-RDAC	20.24	12.27	6.05	12.85	−26.6
Generator speed (MSE)	rpm	ROSCO	943.84	250.37	36.49	410.24	-
		CPC-RDAC	307.94	122.62	30.94	153.83	−62.5
		IPC-RDAC	409.92	150.69	36.6	199.07	−51.5
Generator power (δ)	kW	ROSCO	190.24	104.22	40.12	111.52	-
		CPC-RDAC	304.13	165.74	61.91	177.26	59
		IPC-RDAC	234.45	146.15	60.35	146.98	31.8
Generator power (MSE)	kW	ROSCO	36236	10879	1609.8	16241.6	-
		CPC-RDAC	92497	27473	3833.5	41267.83	154.1
		IPC-RDAC	54966	21360	3642	26656.2	64.1
Pitch travel (Mean)	°	ROSCO	14.251	11.331	7.574	11.052	-
		CPC-RDAC	14.291	11.347	7.578	11.072	0.18
		IPC-RDAC	14.290	11.357	7.577	11.075	0.21

Abbreviations: CPC-RDAC, CPC-based robust disturbance accommodating controller; IPC-RDAC, independent pitch-based robust disturbance accommodating controller; MSE, mean square error; ROSCO, reference open-source controller.

activity compared with ROSCO and CPC-RDAC as shown in Figure 8. However, the graphs of generator speed and power MSE show that the proposed controller strikes a good balance between generator speed and power regulation. Therefore, the proposed controller meets all the control objectives without violating the turbine's PR constraint.

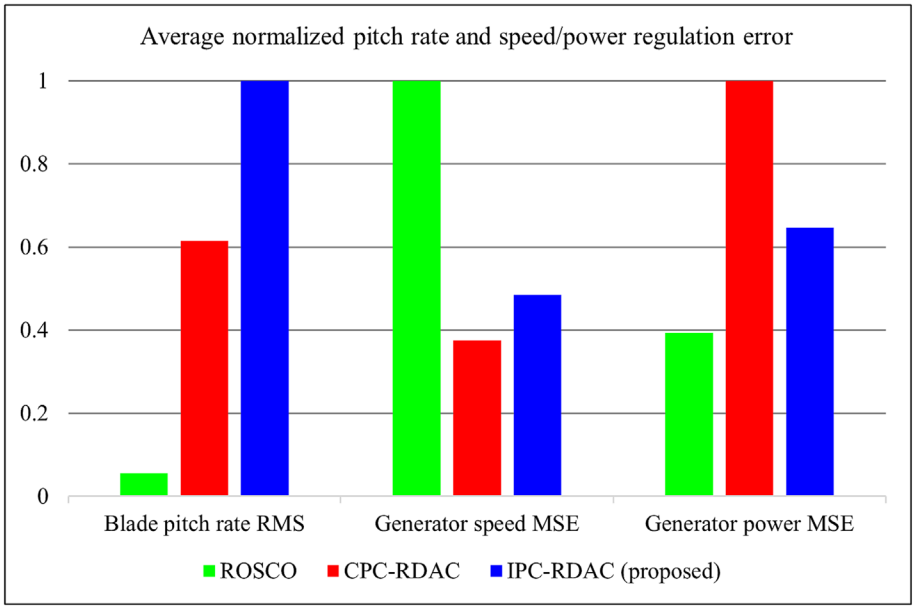

FIGURE 8 Blade pitch activity and generator speed/power regulation error.

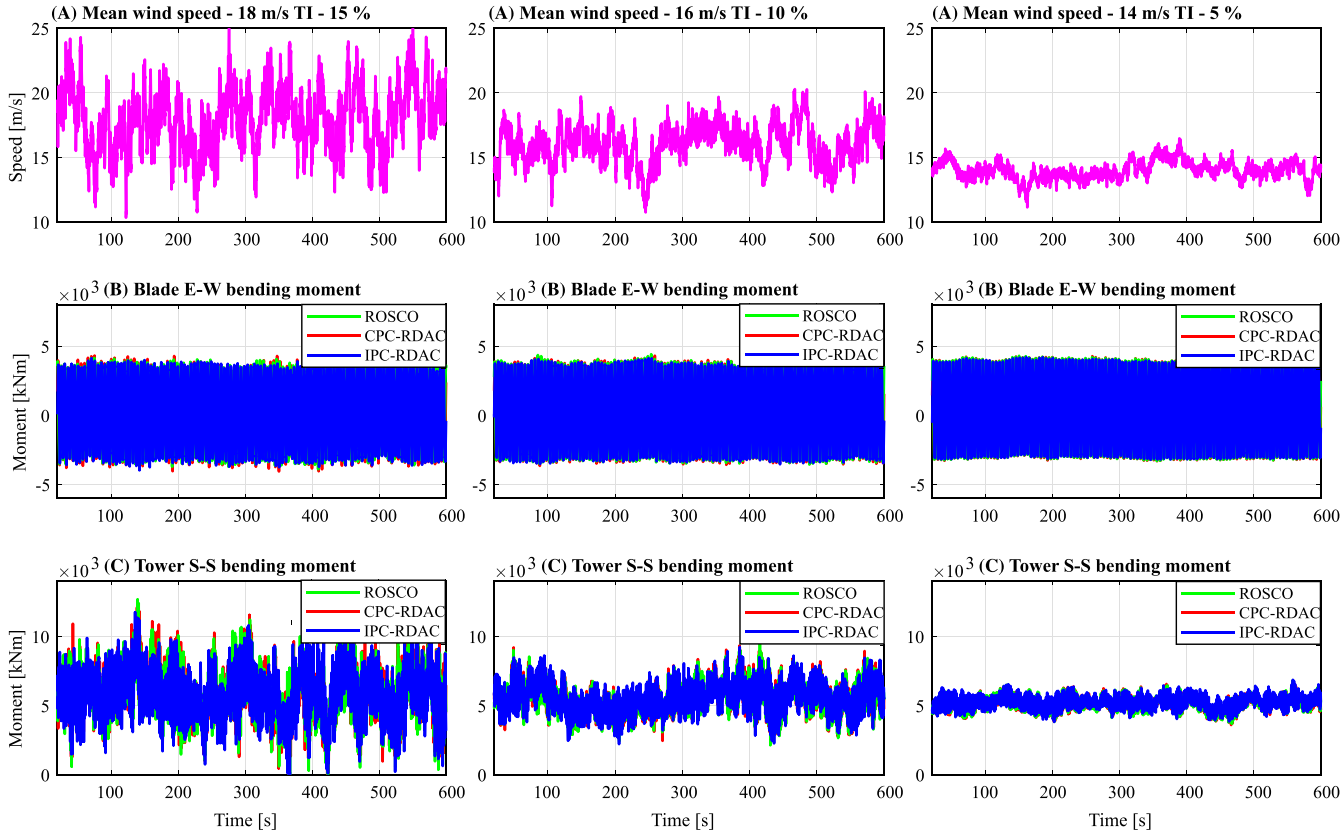

FIGURE 9 (A–C) Blade E-W and tower S-S loading response.

4.3 | Load mitigation in other load channels

Due to coupling between the tower, blades, and drive-train dynamics in a WT, implementing a control scheme for load mitigation in one structural component can result in increased loading in other WT components. For example, the use of IPC control potentially excites the blade edge-wise (E-W)and tower side-side (S-S) bending modes. Therefore, in this contribution, additional load channels in the blades and tower are evaluated as shown in Figure 9. As illustrated, the proposed controller does not excite loading in other load channels for all wind field scenarios. This is shown

in Table 6, as the proposed controller achieves the best performance. Compared with the ROSCO, the average reduction in δ for blade E-W and tower S-S moments is 2.2% and 5.3%, respectively. On the other hand, CPC-RDAC shows a marginal increase in δ for both load channels. Therefore, while the use of CPC-RDAC compromises on performance in other load channels, the IPC-RDAC controller provides an optimal trade-off between load mitigation and generator speed regulation.

4.4 | Fatigue load analysis

The robustness of the proposed controller in fatigue load reduction is examined by conducting damage equivalent loads (DELs) analysis of the respective blades and tower load channels using MLife software.[38] Closed-loop simulation results obtained using the wind profiles shown in Figure 6A are used in this analysis. The wind fields cover most of the WT's above-rated operations. In Figure 10, the normalized DELs with respect to ROSCO for each load channel and in all wind conditions is shown. As illustrated, the blades F-W and E-W DELs are reduced in IPC-RDAC controller compared with ROSCO and CPC-RDAC controllers for all wind fields, with an average reduction of 11.6% and 20.7% for blade F-W DEL, and 1.9% and 2.7% for blade E-W DEL, respectively as shown in Table 7. Additionally, the IPC-RDAC controller shows improvement for the tower F-A DEL compared with both ROSCO and CPC-RDAC, with an average reduction of 6.9%and 2.1%, respectively. However, the proposed controller exhibits a slightly reduced performance in tower S-S DEL as it achieves an average increase of 4.9% and 2.8% compared with ROSCO and CPC-RDAC controllers, respectively. This can be attributed to use of IPC control, which typically excites the tower S-S vibration

TABLE 6 Blade E-W and tower S-S load mitigation performance analysis (Key: best, worst).

Load channel (kNm)	Controller	18 m/s	16 m/s	14 m/s	Avg.	%
Blade E-W moment (δ)	ROSCO	2449.5	2489.1	2516.1	2484.9	-
	CPC-RDAC	2453.7	2487.7	2516.7	2486	0.1
	IPC-RDAC	2393.1	2431.3	2468.0	2430.8	−2.2
Tower S-S moment (δ)	ROSCO	1779.7	1065.7	455	1100.13	-
	CPC-RDAC	1815.7	1076.3	458.42	1116.81	1.5
	IPC-RDAC	1680.6	1023.2	421.8	1041.9	−5.3

Abbreviations: CPC-RDAC, CPC-based robust disturbance accommodating controller; IPC-RDAC, independent pitch-based robust disturbance accommodating controller; MSE, mean square error; ROSCO, reference open-source controller.

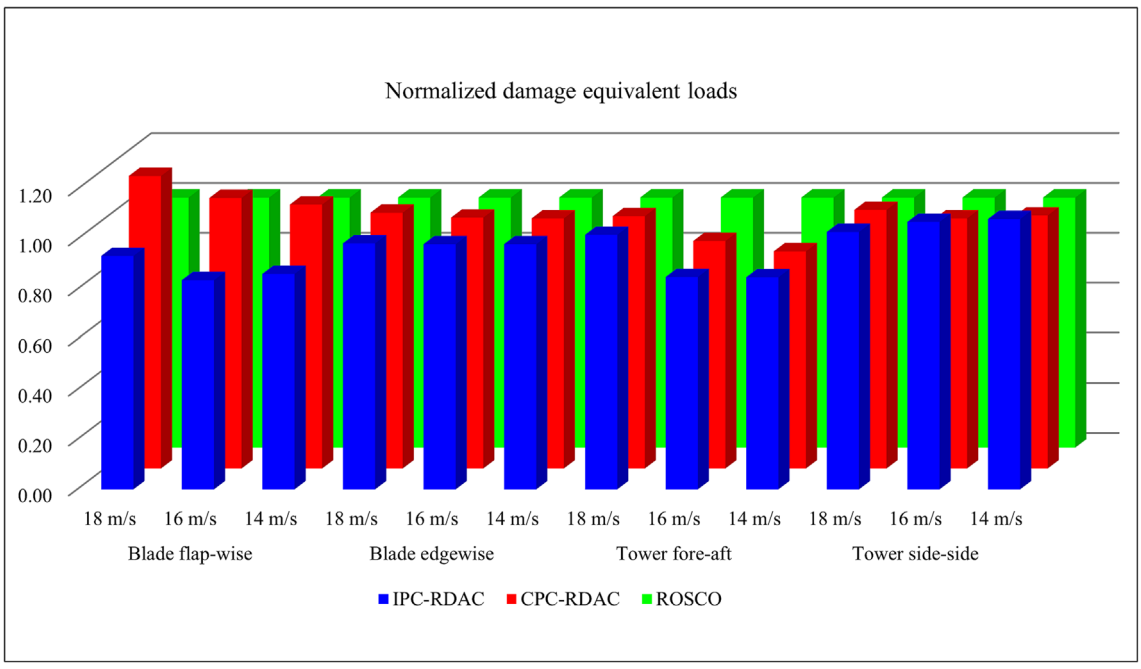

FIGURE 10 Damage equivalent loads analysis.

TABLE 7 Damage equivalent loads analysis (Key: best, worst).

DEL channel (kNm)	Controller	18 m/s	16 m/s	14 m/s	Avg.	%
Blade F-W	ROSCO	3000	2440	1440	2293.3	-
	CPC-RDAC	3510	2640	1520	2556.7	11.5
	IPC-RDAC	2800	2040	1240	2026.7	−11.6
Blade E-W	ROSCO	3050	3060	3060	3056.7	-
	CPC-RDAC	3120	3070	3060	3083.3	0.9
	IPC-RDAC	3000	3000	3000	3000	−1.9
Tower F-A	ROSCO	5590	3970	1970	3843.3	-
	CPC-RDAC	5640	3610	1710	3653.3	−4.9
	IPC-RDAC	5690	3370	1670	3576.7	−6.9
Tower S-S	ROSCO	2050	1150	506	1235.3	-
	CPC-RDAC	2120	1150	512	1260.7	2.1
	IPC-RDAC	2110	1230	547	1295.7	4.9

Abbreviations: CPC-RDAC, CPC-based robust disturbance accommodating controller; DEL, damage equivalent load; IPC-RDAC, independent pitch-based robust disturbance accommodating controller; MSE, mean square error; ROSCO, reference open-source controller.

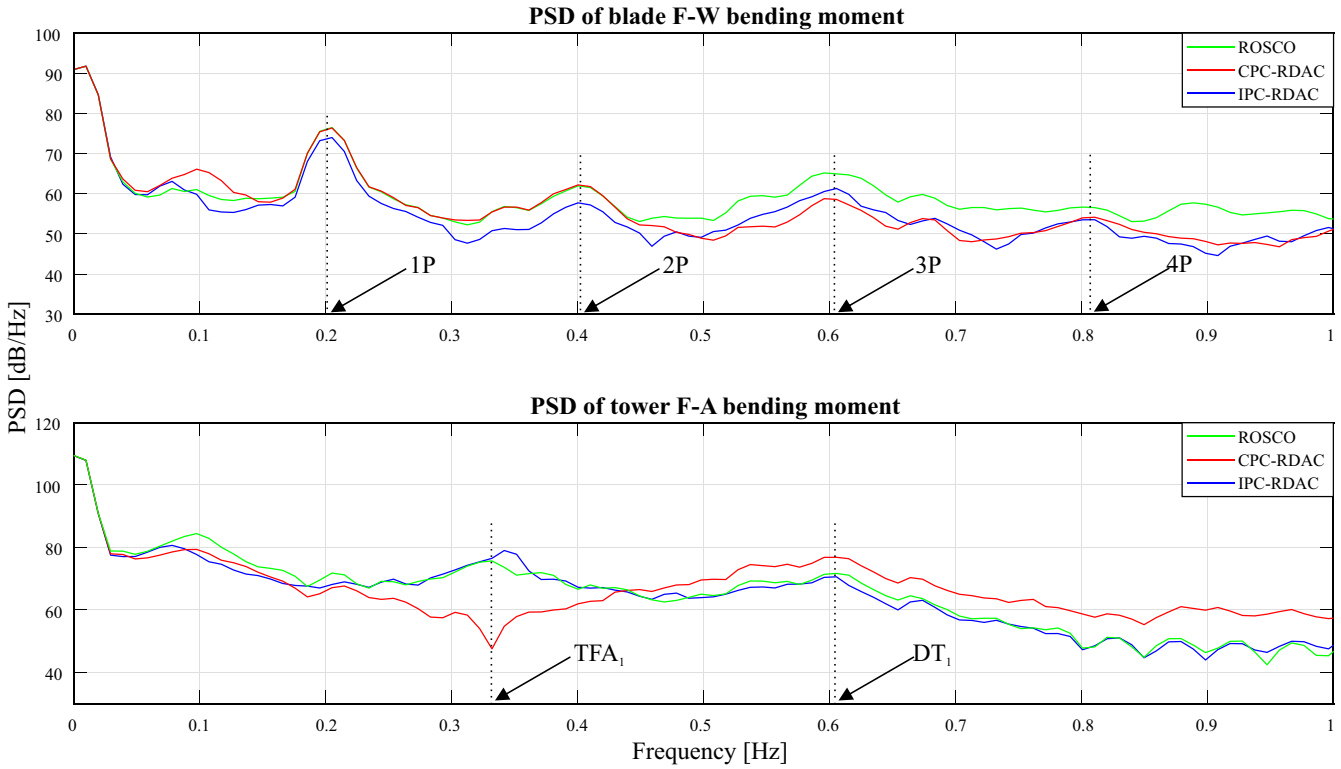

FIGURE 11 Power spectral density analysis of blade F-W and tower F-A bending moments.

mode. However, the performance of the proposed controller in mitigating structural loads in most load channels and aforementioned optimal performance in generator speed and power regulation far outweighs this setback. Therefore, the IPC-RDAC controller offers optimal balance in fatigue load reduction and generator speed regulation.

4.5 | Spectral analysis

To evaluate the performance of controllers in alleviating structural loads at frequencies of interest, power spectral density (PSD) analysis of the blade F-W and tower F-A bending moments is performed. In Figure 11, the results of the PSD evaluation are shown. As illustrated, the IPC-RDAC

controller gives the lowest response peak magnitudes of blade F-W loading at 2P and 4P frequencies as compared with ROSCO and CPC-RDAC controllers. This means that the proposed controller alleviates the asymmetrical blade F-W bending moments, ζ_{tilt} and ζ_{yaw}. This is because dynamic coupling of blade F-W bending modes, $\zeta_{avg}, \zeta_{tilt}$, and ζ_{yaw} is considered in controller design by proper selection of weighting functions as discussed in Section 3.4.2. Furthermore, the IPC-RDAC controller achieves better 3P blade load reduction (related to ζ_{avg}) compared with ROSCO. Although 1P is far from the critical natural frequencies of the blades (around 4 rad/s) and the tower (2.07 rad/s) shown in Table 3, its higher-order harmonics contribute to excitation of these frequencies. Therefore, only reduction of 2P, 3P, and 4P frequencies are considered in the design of the proposed controller. Further suppression of 1P blade excitation can additionally be considered by designing W_{13} and W_{14} with high magnitudes near 0P frequency. The CPC-RDAC controller has superior performance in suppressing blade vibration at 3P, which is accounted for in its design as it indirectly reduces 3P blade excitation experienced at tower. This is illustrated in the tower F-A PSD analysis, in which CPC-RDAC damps tower F-A loading at the first tower bending moment TFA_1 frequency. Although the proposed controller does not show reduced damping at this frequency, it achieves lower magnitude response in tower loading at higher frequencies compared with CPC-RDAC. In particular, it shows less tower loading at the first drive-train torsional frequency DT_1, indicating that the use of IPC-RDAC leads to lower excitation of the coupled drive-train dynamics.

5 | SUMMARY, CONCLUSIONS, AND OUTLOOK

In this contribution, a robust disturbance accommodating controller based on IPC control for structural load mitigation and generator speed regulation of the 5 MW NREL RWT is outlined. The novel IPC-RDAC controller is designed using μ-synthesis based on the *DK*-iteration process by minimizing the structured singular value μ of the generalized WT system made up of a linear model, weighting functions, and blade pitch actuator dynamics. The controller also includes an uncertainty description, which is designed from a family of linear models obtained at different operating points. Periodic 2P,3P, and 4P frequencies as well as the first tower fore-aft frequency reflected in the rotor blades are reduced by designing the respective weighting functions. The proposed controller is shown by suitable simulations to be robust against model uncertainties and system nonlinearities resulting from wind speed variability. Compared with baseline ROSCO and CPC-RDAC controllers, dynamic simulation results show that the proposed controller reduces fatigue loading in the blades and tower without compromising on the generator speed regulation performance. It also exhibits reduced loading in other WT load channels. Fatigue load evaluation indicates a reduction of DELs in most load channels.

The limitation of this work is that only unstructured uncertainties have been considered in the uncertainty description. Additionally, the blade pitch actuator activity is aggressive especially in wind fields having high speeds and TIs. However, these wind conditions have a low occurrence probability in a real-world operation of WTs and have been used to show the effectiveness of the proposed controller in the event that such conditions arise. This work can be extended designing the relevant weighting functions to further reduce 1P frequencies in the blades. A lumped uncertainty description, which incorporates additionally plant parametric uncertainties experienced especially in below-rated WT operation, can be included to potentially improve RP. A prognostics-based IPC-RDAC lifetime controller can also be developed with the view of controlling long-term fatigue damage accumulation in WT structural components.

ACKNOWLEDGEMENTS

The research reported in this paper is partly supported through a scholarship awarded to the first author by the German Academic Exchange Service (DAAD) in cooperation with the Ministry of Education of Kenya, for his Ph.D. study at the Chair of Dynamics and Control, UDE, Germany. Open Access funding enabled and organized by Projekt DEAL.

CONFLICT OF INTEREST STATEMENT

The authors declare no potential conflict of interests.

PEER REVIEW

The peer review history for this article is available at https://www.webofscience.com/api/gateway/wos/peer-review/10.1002/we.2893.

DATA AVAILABILITY STATEMENT

The data that support the findings of this study are available from the corresponding author upon reasonable request.

ORCID

Edwin Kipchirchir https://orcid.org/0000-0002-5567-7225

REFERENCES

1. Gielen D, Gorini R, Leme R, Prakash G. World energy transitions outlook: 1.5°C pathway (preview), International Renewable Energy Agency (IRENA); 2021.

2. Lee J, Zhao F. Global wind report 2021, Global Wind Energy Council (GWEC); 2021. https://gwec.net/global-wind-report-2021/
3. Lee J, Zhao F. GWEC | Global wind report 2019, Global Wind Energy Council (GWEC); 2020. https://gwec.net/global-wind-report-2019/
4. Abbas NJ, Zalkind DS, Pao L, Wright A. A reference open-source controller for fixed and floating offshore wind turbines. *Wind Energy Sci Discuss*. 2021;2021:1-3. https://doi.org/10.5194/wes-2021-19
5. Geyler M, Caselitz P. Robust multivariable pitch control design for load reduction on large wind turbines. *J Sol Energy Eng Trans ASME*. 2008;130(3): 0310141-03101412. https://doi.org/10.1115/1.2931510
6. Yuan Y, Chen X, Tang J. Multivariable robust blade pitch control design to reject periodic loads on wind turbines. *Renew Energy*. 2020;146:329-341. https://doi.org/10.1016/j.renene.2019.06.136
7. Wang N, Wright AD, Johnson KE. Independent Blade Pitch Controller Design for a Three-Bladed Turbine Using Disturbance Accommodating Control. *2016 American Control Conference (ACC)*. Boston, MA, USA: IEEE. 2016:2301-2306.https://doi.org/10.1109/ACC.2016.7525261
8. Wang N, Wright AD, Balas MJ. Disturbance accommodating control design for wind turbines using solvability conditions. *J Dyn Syst Meas Control*. 2017;139(4):41007. https://doi.org/10.1115/1.4035097
9. Menezes EJN, Araujo AM, Rohatgi JS, del Foyo PMG. Active load control of large wind turbines using state-space methods and disturbance accommodating control. *Energy*. 2018;150:310-319. https://doi.org/10.1016/j.energy.2018.02.143
10. Cheon J, Kwon S, Choi Y. Design of a pitch controller using disturbance accommodating control for wind turbines under stochastic environments. *IEEE 23rd International Symposium on Industrial Electronics (ISIE)*. Istanbul, Turkey: IEEE; 2014:2572-2577. https://doi.org/10.1109/ISIE.2014.6865025
11. Corcuera AD, Pujana-arrese A, Nourdine S, Camblong H, Landaluze J. GH bladed's linear models based H_∞ controls for off-shore wind turbines. In: Offshore 2011; 2011.
12. Corcuera AD, Pujana-arrese A, Ezquerra JM, Segurola E, Landaluze J. H_∞ based control for load mitigation in wind turbines. *MDPI-energies*. 2012;5: 938-967.https://doi.org/10.3390/en5040938
13. Poureh A, Nobakhti A. Robust control design for an industrial wind turbine with HIL simulations. *ISA Trans*. 2020;103:252-265. https://doi.org/10.1016/j.isatra.2020.05.004
14. Mihaly V, Susca M, Morar D, Dobra P. μ-synthesis for fractional-order robust controllers. *MDPI-Mathematics*. 2021. https://doi.org/10.3390/math9080911
15. Mirzaei M, Niemann HH, Poulsen NK. A μ-synthesis approach to robust control of a wind turbine. In: Proceedings of the IEEE Conference on Decision and Control and European Control Conference; 2011; Orlando, Florida: 645-650. https://doi.org/10.1109/CDC.2011.6161124
16. Park S. A novel individual pitch control algorithm based on μ-synthesis for wind turbines. *J Mech Sci Technol*. 2014;28(4):1509-1517. https://doi.org/10.1007/s12206-014-0138-y
17. Moradi H, Vossoughi G. Robust control of the variable speed wind turbines in the presence of uncertainties: a comparison between H_∞ and PID controllers. *Energy*. 2015;90:1508-1521. https://doi.org/10.1016/j.energy.2015.06.100
18. Zhang C, Tahoumi E, Gutierrez S, Plestan F, Deleon-Morales J. Adaptive robust control of floating offshore wind turbine based on sliding mode. In: IEEE 58TH Conference on Decision and Control (CDC); 2019; Nice, France: 6936-6941. https://doi.org/10.1109/CDC40024.2019.9029231
19. Azizi A, Nourisola H, Shoja-Majidabad S. Fault tolerant control of wind turbines with an adaptive output feedback sliding mode controller. *Renew Energy*. 2019;135:55-65. https://doi.org/10.1016/j.renene.2018.11.106
20. Nayeh RF, Moradi H, Vossoughi G. Multivariable robust control of a horizontal wind turbine under various operating modes and uncertainties: a comparison on sliding mode and H_∞ control. *Electr Power Energy Syst*. 2020;115:105474. https://doi.org/10.1016/j.ijepes.2019.105474
21. Do MH, Söffker D. Robust observer-based load extenuation control for wind turbines. *ASME 2019 IDETC-CIE 2019*. Anaheim, CA: ASME; 2019. https://doi.org/10.1115/DETC2019-97645
22. Do MH, Söffker D. Wind turbine robust disturbance accommodating control using non-smooth H_∞ optimization. *Wind Energy*. 2022;25:107-124. https://doi.org/10.1002/we.2663
23. Kipchirchir E, Do MH, Njiri JG, Dirk S. Mixed-sensitivity robust disturbance accommodating control for load mitigation and speed regulation of wind turbines. In: 2022 European Control Conference (ECC). IEEE; 2022; London, United Kingdom: 1012-1017. https://doi.org/10.23919/ECC55457.2022.9838131
24. Bir G. User's guide to MBC3: multi-blade coordinate transformation code for 3-bladed wind turbines. NREL/TP-500-44327, National Renewable Energy Laboratory (NREL); 2010. https://www.nrel.gov/docs/fy10osti/44327.pdf
25. Jonkman J, Butterfield S, Musial W, Scott G. Definition of a 5-MW reference wind turbine for offshore system development. NREL/TP-500-38060, Golden, Colorado, National Renewable Energy Laboratory (NREL); 2009. https://www.nrel.gov/docs/fy09osti/38060.pdf
26. Rinker J, Gaertner E, Zahle F, Abbas N, Bredmose H, Barter G. Comparison of loads from HAWC2 and OpenFAST for the IEA wind 15 MW reference wind turbine. *Journal of Physics: Conference Series*, Vol. 1618: IOP Publishing Ltd.; 2020. https://doi.org/10.1088/1742-6596/1618/5/052052
27. NREL. OpenFAST documentation, National Renewable Energy Laboratory (NREL); 2021.
28. Apkarian P, Noll D. Nonsmooth H_∞ synthesis. *IEEE Trans Autom Control*. 2006;51(1):71-86. https://doi.org/10.1109/TAC.2005.860290
29. Apkarian P, Noll D. The H_∞ control problem is solved. *AerospaceLab*. 2017;13:1-13. https://doi.org/10.12762/2017.AL13-01
30. Wright AD. Modern control design for flexible wind turbines. NREL/TP-500-35816, Golden, Colorado; 2004. https://www.nrel.gov/docs/fy04osti/35816.pdf
31. Wright AD, Fingersh LJ. Advanced control design for wind turbines part I: control design, implementation, and initial tests. NREL/TP-500-42437, Golden, Colorado, National Renewable Energy Laboratory (NREL); 2008. https://www.nrel.gov/docs/fy08osti/42437.pdf
32. Fingersh LJ, Johnson KE. Baseline results and future plans for the NREL controls advanced research turbine. In: 42nd AIAA Aerospace Sciences Meeting and Exhibit; 2004; Reno, Nevada. https://doi.org/10.2514/6.2004-347
33. Söffker D, Yu T, Müller PC. State estimation of dynamical systems with nonlinearities by using proportional-integral observer. *Int J Syst Sci*. 1995; 26(9):1571-1582. https://doi.org/10.1080/00207729508929120
34. Apkarian P. Nonsmooth μ-synthesis. *Int J Robust Nonlinear Control*. 2011;21:1493-1508. https://doi.org/10.1002/rnc.1644
35. Rinker J, Dykes K. WindPACT reference wind turbines. NREL/TP-5000-67667, Golden, Colorado, National Renewable Energy Laboratory (NREL); 2018. https://www.nrel.gov/docs/fy18osti/67667.pdf
36. Skogestad S, Postlethwaite I. *Multivariable Feedback Control Analysis and Design*: John Wiley and Sons; 2005.

37. Jonkman B, Kilcher L. TurbSim user's guide: version 1.50. NREL/TP-500-46198, Golden, Colorado, National Renewable Energy Laboratory (NREL); 2009. https://www.nrel.gov/docs/fy09osti/46198.pdf
38. Hayman GJ. MLife theory manual for version 1.00, Golden, Colorado, National Renewable Energy Laboratory(NREL); 2012. https://www.nrel.gov/wind/nwtc/assets/pdfs/mlife-theory.pdf

How to cite this article: Kipchirchir E, Söffker D. IPC-based robust disturbance accommodating control for load mitigation and speed regulation of wind turbines. *Wind Energy*. 2024;1-21. doi:10.1002/we.2893